SURFACE STICKING PROBABILITIES FOR SPUTTERED ATOMS OF ^{93}Nb AND ^{103}Rh[†]

MARTHA RIHERD WELLER[‡] and T. A. TOMBRELLO

W. K. Kellogg Radiation Laboratory, California Institute of Technology

Pasadena, California 91125

[†]Supported in part by the Department of Energy [EY-76-G-03-1305], the National Science Foundation [PHY 76-83685], and the National Aeronautics and Space Administration [NGR-05-002-333].

[‡]Present address: Naval Research Laboratory, Code 6673; Washington, D.C. 20390.

ABSTRACT

The sticking probabilities for sputtered atoms of ^{93}Nb and ^{103}Rh incident on Al_2O_3 surfaces have been measured using the backscattering of MeV heavy ions. In the circumstance where the collecting surface has become thickly covered, the sticking probabilities integrated over the energy distribution of sputtered atoms are 0.97 ± 0.01 and 0.95 ± 0.01 for ^{93}Nb and ^{103}Rh, respectively. In the limit of negligible areal coverage of the collector, the accuracy is less; in this case the sticking probabilities are $0.97^{+0.03}_{-0.08}$ and $0.95^{+0.05}_{-0.08}$.

1. INTRODUCTION

Determination of sticking probabilities for atoms incident on solid surfaces and analysis of the scattered atoms are of considerable interest for several reasons. Sticking probabilities (synonymous with trapping fraction and capture coefficient) are expected to depend strongly on the atom-surface interaction and models for this interaction can be checked by comparing experimental sticking data with the model predictions (see, e.g., Modak and Pagni,[1] Trilling and Hurkmans[2]). Such measurements are also important in connection with sputtering measurements which involve collection of sputtered material. There the sticking probability is a necessary ingredient in determining the sputtering yields. Finally, the growth of grains in interstellar space, and hence the composition, is strongly influenced by atomic sticking probabilities.

In general, sticking probability measurements have been restricted to a few small classes of atom-surface combinations: Most measurements have involved rare gases or alkali metals incident on metallic (usually tungsten) surfaces (Hurkmans et al.,[3,4] Sau and Merrill[5]), although there have also been a few measurements for alkali metals on ionic crystals (Tomoda et al.[6]). Measurements involving other atom-surface combinations include silver on tungsten (Cho and Hendricks[7]) and uranium on Al_2O_3 and gold (Libbrecht et al.[8]).

For the applications mentioned earlier, it would be useful to know the sticking probabilities for a greater variety of atom-surface combinations. In this paper we describe a technique for measuring sticking factors which is relatively independent of the chemical properties of the incident atoms and surfaces involved and thus may be used for a wider range of atom-surface combinations.

2. EXPERIMENTAL PROCEDURE

Our technique for determining sticking factors is a modification of the "double-bounce" technique used by Libbrecht et al.[8] to determine the sticking probability for uranium atoms sputtered onto a surface of Al_2O_3. In this section, we give a brief overview of the technique, followed by a more detailed description of the sputtering and analysis procedures.

2.1 Overview

As shown in Figure 1, low energy atoms are produced by sputtering a target of material A. As the sputtered atoms enter the sticking factor chamber, they are collimated into a "beam" which has radius a at the surface of the primary catcher foil (material B). Atoms incident on this foil stick with probability $k_B^A(n_1(r))$ where $n_1(r)$ is the surface density of atoms of A on the primary foil as a function of the distance r from the center of the beam spot. Sputtered atoms which do not stick to the primary foil may be scattered onto the cylindrical secondary catcher foil (also of material B) where they stick with probability $k_B^A(n_2(\chi))$ [$n_2(\chi)$ is the surface density of atoms of A on the secondary foil at the angle χ]. If the surface densities $n_1(r)$ and $n_2(\chi)$ are sufficiently small (much less than a monolayer), k_B^A should be independent of the thickness of deposited material A. If it is also assumed that, at low energies, k_B^A does not vary as a function of incident energy (or, alternatively, that the energy spectra of the incident particles are the same for both catcher foils), the sticking factor may be determined by measuring the surface densities $n_1(r)$ and $n_2(\chi)$. These densities are related to the sticking factor by

$$k_B^A = 1 - R^2 \frac{\int_0^{\pi/2} n_2(\chi) \sin\chi \, d\chi}{\int_0^a n_1(r) \, r \, dr} \qquad (1)$$

where R is the radius of the secondary catcher foil. The measurement by Libbrecht et al.[8] suggests that, at least for heavy atoms incident on a light substrate, the assumption about the energy dependence of k_B^A is valid.

The nuclear track technique used by Libbrecht et al.[8] for determining uranium surface thicknesses is sufficiently sensitive that Equation (1) may be used to determine k_B^A. However, for most surface analysis techniques, $n_1(r)$ must be several monolayers in order to measure $n_2(\chi)$ if k_B^A is close to 1. Thus, the assumption that k_B^A is independent of thickness may be invalid and Equation (1) must be modified. In order to do this, it is useful to define two quantities. If a thickness n of sputtered material is collected on an initially clean catcher foil, the ratio of collected atoms to incident atoms is given by:

$$K_B^A(n) = \left[\frac{1}{n}\int_o^n \frac{dn'}{k_B^A(n')}\right]^{-1} . \qquad (2)$$

We also define the relative sticking factor, $k_B^A(n) = K_B^A(n)/K_B^A(0)$. In the limit of small n, $K_B^A(n) = k_B^A(n)$ and $k_B^A(n) = 1$. For large n, we expect $K_B^A(n) = K_A^A(n) = k_A^A(n) =$ constant. If $n_2(\chi)$ is sufficiently small for all χ and if $n_1(r)$ is sufficiently large so that $k_B^A(n_2(\chi)) = 1$ and $K_B^A(n_1(r))$ is constant for all r, then $k_B^A(0)$ may be determined if we also assume that the angular distribution of the atoms scattered from the primary foil is independent of $n_1(r)$. We find

$$k_B^A(0) = \frac{1}{k_B^A(n_1)} - R^2 \frac{\int_o^{\pi/2} n_2(\chi)\sin\chi\, d\chi}{\int_o^a n_1(r)\, r\, dr} . \qquad (3)$$

Equation (3) differs only slightly from Equation (1): In order to determine $k_B^A(0)$, we must measure not only the thicknesses $n_1(r)$ and $n_2(\chi)$, but also the relative sticking factor $k_B^A(n_1)$.

The relative sticking factor may be determined using the geometry shown in Figure 2. After the target is sputtered, the final distribution of collected material on the catcher foil is given by

$$n(\theta) = \frac{S(\theta)}{D^2} K_B^A(n(\theta)) \frac{Q}{q} . \qquad (4)$$

In this equation, $S(\theta)$ is the differential sputtering yield, D is the radius of the catcher foil, q is the charge of the incident sputtering ion, and Q is the final integrated charge of these ions. By comparing the distributions, $n_i(\theta)$, obtained from various integrated charges, Q_i, the relative sticking factor may be determined. In particular, if n_o is small enough that $K_B^A(n_o) = K_B^A(0)$, then we find

$$k_B^A(n_i) = \frac{n_i(\theta)}{n_o(\theta)} \frac{Q_o}{Q_i} . \qquad (5)$$

Once the sputtered material has been collected, the surface thicknesses must be determined before Equations (3) and (5) may be used. For our measurements, these thicknesses were determined by Rutherford backscattering with ^{19}F or ^{16}O ions.

2.2 The Sputtering Runs

As indicated above, two sputtering runs were necessary for each sticking factor determination. For all of these runs, the target was sputtered with 80 keV $^{40}Ar^+$ ions and the sputtered material was collected on catcher foils which were 99.997% aluminum. Since aluminum forms a thin protective oxide

layer when exposed to the atmosphere, the catcher foil surface itself was Al_2O_3. The targets were thick foils of pure niobium or pure rhodium which were at room temperature.

All sputtering runs were carried out in an ultra-high vacuum (UHV) system which had a base pressure of $\sim 2 \times 10^{-9}$ Torr. At such pressures, the catcher foils would be coated with a layer of gas atoms. This could affect the sticking factor for the sputtered atoms and will be discussed later. When the $^{40}Ar^+$ sputtering beam was introduced into the UHV system, the pressure rapidly rose to an equilibrium value of $\sim 10^{-6}$ Torr. Fortunately, inert gases are not strongly adsorbed so this increased pressure probably did not affect the surface of the catcher foils. It was also not high enough to cause scattering of the sputtered atoms or otherwise affect the sputtering process.

The first sputtering run was performed using the catcher foil geometry shown in Figure 2. A large catcher foil was mounted on a vertically movable cylinder which had a radius of 3.8 cm. A fixed masking cylinder was placed between the target and the catcher foil cylinder so that only the region of the catcher foil which was at beam level collected sputtered material. Thus, by moving the catcher foil cylinder vertically, several distributions, $n_i(\theta)$, could be obtained without breaking the vacuum.

As can be seen from Equation (5), it was important that the current due to the sputtering beam be integrated correctly. The beam was collimated upstream to a diameter of ~ 3 mm so that it reached the target without striking either the catcher foil cylinder or the masking cylinder. The two cylinders were electrically connected to the target so that the net current from the entire assembly was integrated. Thus, the target bias should not have affected the measured current since most of the secondary electrons produced at the target were trapped by the cylinders surrounding it. We found no change in

the current when the bias was changed from +300 V to -300 V. During the actual run, the target bias was +300 V.

It was also necessary that the sputtering yield, $S(\theta)$, be the same for all of the distributions $n_i(\theta)$. In particular, the surface of the target could not change after we began to collect sputtered material. We also wanted other parameters such as the UHV pressure to remain constant. Both of these conditions were satisfied by sputter-cleaning the target with a 5-μA $^{40}Ar^+$ beam for about half an hour prior to collection of the sputtered material. This was enough to remove any surface oxide layer on the target, establish an equilibrium Ar distribution within the target, and also raise the pressure to its equilibrium value of $\sim 10^{-6}$ Torr.

After the target had been sputter-cleaned, the catcher foil was exposed to the target and sputtered material was collected until an integrated charge of Q_1 was reached. The beam was then deflected and a clean region of catcher foil was exposed to the target. This procedure was repeated for several integrated charges, Q_i, ranging from 1×10^{-3} C to 2×10^{-2} C for the Nb measurement and from 6×10^{-4} C to 1.8×10^{-2} C for the Rh measurement. In all cases, the integrated charges were the same for the first and last distributions collected during each run in order to determine the reproducibility of the distributions.

Once the sputtering run was completed, the catcher foils were removed from the UHV system and stored for later analysis.

The second sputtering run was performed using the geometry of Figure 1. Catcher foils were mounted in two sticking factor chambers and clamped into position as shown. The radius of the secondary catcher foil was 1.27 cm and the diameter of the entrance hole to each chamber was 3.2 mm.

For this run, it was not possible to shield the catcher foils from the target until the equilibrium conditions discussed above were established. However, in order to collect enough material on the secondary foil to permit analysis, it was necessary to run for an integrated charge of $Q \gtrsim 0.5$ C. Since equilibrium conditions were reached after a much shorter integrated charge, the lack of shielding was not expected to affect the results of this run.

Accurate current integration was not crucial for this run. The current was monitored primarily to determine when enough material had been sputtered, although we also tried to reproduce the average current used in the first sputtering run. When the desired integrated charge was reached, the catcher foils were removed from the UHV system and stored for analysis.

2.3 Catcher Foil Analysis

Once the sputtering runs were completed, the surface thicknesses were determined by Rutherford backscattering analysis with 10-MeV ^{19}F or ^{16}O ions. In the mass region near $A \approx 100$, surface thicknesses as low as 5×10^{13} atoms/cm^2 can be measured easily with this technique. The sensitivity increases at lower beam energies, but we observed significant target sputtering at energies much below 10 MeV. Since we were using a Si surface barrier detector to detect the backscattered ions, our mass resolution was not good. However, that was not important for this measurement since the mass of the scattering nuclei was known and since there was no foil contaminant in the relevant mass region.

The catcher foils were mounted on a hexagonal target holder and placed in the scattering chamber as shown in Figure 3. The target holder was attached to a vertical feed-through which allowed it to be raised, lowered or rotated from outside the chamber. A quartz slide was also mounted on the target holder

to allow visual monitoring and adjustment of the size and shape of the ion beam. The beam spot was always smaller than 2 mm on a side. Typical beam currents were 100 nA.

For heavy ion beams such as ^{19}F and ^{16}O, current integration can be a problem due to secondary electrons (Loebenstein et al.[9]). The current was integrated from the target which was biased at +1200 V and the beam was collimated upstream so that electrons from the collimation slits did not reach the target. By observing the backscattered yield at several energies, we verified that the current integration did not vary with beam energy. Since the secondary electron production changes with the incident beam energy, this indicated that our electron suppression was adequate.

As shown in Figure 3, the detector was located at an angle of 147.8^{o} relative to the incident beam. It subtended a solid angle of 6.0×10^{-3} sr. Pulses from the detector were amplified and counted using a multi-channel analyzer. The yield of backscattered particles could then be used to determine the surface thickness of sputtered material in the region of the beam spot.

For this experiment, the most important problem and probably the largest source of error was in the positioning of the foils. To determine the relative sticking factor from Equation (5), it was necessary to measure the surface thickness of sputtered material at the same value of θ on several foils. To determine the absolute sticking factor from Equation (3), data points taken from the primary and secondary foils had to be correlated with the appropriate values of r and χ, respectively. For the relative sticking factor measurements, the catcher foil was marked prior to the sputtering run. By careful mounting of the various strips of sputtered material on different sides of the target holder, we were able to reproduce θ to within $\Delta\theta = 3.6^{o}$. Comparison of the

distributions on the two foils which had collected sputtered material for the same integrated charge were consistent with this estimate. For the absolute sticking factor measurements, relative positions on the foils could be determined to ± 0.5 mm. Zeros for both r and χ were obtained from the measured thickness distributions by requiring that they be symmetric about r = 0 and χ = 0, respectively.

Once the relevant thickness measurements were correlated with their coordinates during the sputtering runs, the relative and absolute sticking factors could be determined from Equations (3) and (5).

3. RESULTS

Figures 4 and 5 show the relative sticking factors, $k_B^A(n)$, as a function of surface thickness for rhodium and niobium atoms sputtered into surfaces of Al_2O_3. As indicated in the previous section, the major source of error for these measurements was the uncertainty in the foil positions during collection and subsequent analysis. The effects of this uncertainty as well as the effects of possible changes in the target and catcher foil surfaces during the sputtering run were estimated by comparing the spectra, $n_1(\theta)$, obtained from two catcher foils corresponding to the same charge, Q_1, of sputtering ions. Other sources of error (i.e., counting statistics) were much smaller and the total uncertainty for both data sets is estimated at ± 8%.

For both Rh and Nb, there does not seem to be any systematic variation in the sticking factor as a function of the thickness of deposited material. Since such changes should be obvious for thicknesses of a few monolayers, we assume that the sticking factor remains approximately constant and we take $k^{Rh}_{Al_2O_3}(n) = k^{Nb}_{Al_2O_3}(n) = 1.00 \pm 0.08$ for all n.

Absolute sticking factors were also determined for Rh and Nb atoms sputtered onto Al_2O_3 surfaces. As indicated in the previous section, this required measurement of the thickness distributions $n_1(r)$ and $n_2(\chi)$ and evaluation of the integrals $I_1 = \int_0^a n_1(r)\, r\, dr$ and $I_2 = R^2 \int_0^{\pi/2} n_2(\chi) \sin\chi\, d\chi$. Figures 6 and 7 show the distributions obtained for the Rh measurements. Similar results were obtained for Nb. To obtain the integral I_1, the distribution $n_1(r)$ was fitted to a polynomial in r^2. For the integral I_2, $n_2(\chi)$ was fitted to a function of the form $A \cos^m\chi$. For this distribution, some data points (i.e., near the hole in the foil at $\chi = 0^o$) seemed questionable and their inclusion changed the values of A and m significantly from those obtained without these data. However, the integral was not significantly affected. All data points are included in Figures 6 and 7.

Table I shows the values of I_1, I_2, I_2/I_1 and $k_B^A(0)$ as determined from the Rh and Nb measurements. The errors are not symmetric about the values of $k_B^A(0)$ since $k_B^A(0)$ cannot be greater than 1. It should also be noted that the error in $k_B^A(0)$ arises almost entirely from the error in $k_B^A(n)$.

Under some circumstances, the quantity $k_A^A(n)$ can be determined much more accurately than $k_B^A(0)$. In particular, if $n_1(r)$ is large enough for all r such that $k_B^A(n_1)$ satisfies

$$k_B^A(n_1) \approx K_B^A(n_1) \approx k_A^A(n_1),$$

then it can be shown that

$$k_A^A(n_1) = 1 - k_B^A(n_1)\, \frac{I_2}{I_1}.$$

We expect this expression to be valid for both the Rh and Nb measurements. The resulting values for k_A^A are given in the last column of Table I.

At this point, it is important to recall the pressure at which these measurements were made. During the sputtering procedure, the base pressure of the UHV system was $\sim 2 \times 10^{-9}$ Torr, implying that the catcher foil surfaces were initially coated with gas molecules. Thus, we have not really measured the sticking factors for Rh and Nb on an Al_2O_3 surface. Rather, we have measured the sticking factor for these elements on a gas-coated Al_2O_3 surface. The pressure also affected the measurement of relative sticking factors and the determination of k_{Rh}^{Rh} and k_{Nb}^{Nb}. Here the effect was a little more complicated since, for the relative sticking factor measurement and for the primary catcher foil, sputtered material was being deposited more rapidly than gas atoms were being adsorbed onto the surface. What we have really measured in this case are the absolute sticking factors of Rh (or Nb) on the appropriate equilibrium surface mixture of Rh (or Nb) and gas atoms. The relative sticking factor measurements correspond, in fact, to several different mixtures of sputtered atoms and adsorbed gas since sputtered material was deposited at a different rate for each value of θ in Equations (4) and (5). Systematic variations of the sticking factor with θ were not observed for either the Nb or the Rh measurements.

4. DISCUSSION

Most theoretical predictions of sticking factors are obtained from models which consider only the initial collision between the incident atom and surface atoms. If the mass ratio between these atoms is equal to or greater than one and if normal incidence is assumed, all of these models predict sticking factors of unity, independent of specific assumptions about atom-surface interactions. Our results for medium-mass atoms (Rh, Nb) incident on a light surface (Al_2O_3 or the surface gas layer) are consistent with these predictions.

Other authors (Hurkmans et al.,[10] Overbosch et al.[11]) have reported significantly enhanced sticking factors for various ions incident on oxygen-coated tungsten surfaces as compared to the values on clean surfaces. These results support the assumption that only the initial atom-surface collision is important in estimating sticking factors and suggest that little can be learned about atom-surface interactions for cases where the mass ratio is greater than one.

Other results contradict the predictions of the single collision models. For example, our results which are described herein show that in two cases where the mass ratio is exactly one, the sticking factor is slightly, but significantly, less than one. Similar results have been obtained by Libbrecht et al.[8] for sputtered uranium atoms incident on surfaces of Al_2O_3 and Au. For the uranium measurements, resputtering of the deposited uranium atoms was eliminated as a source of the discrepancy (Libbrecht et al.[8]); this effect also seems unlikely in our experiments. It is improbable that thermal processes are responsible since the measurements were made at relatively low temperatures ($\sim 300\ ^{o}K$); also, the angular distribution of material deposited on the secondary foil is inconsistent with such processes. A more likely possibility is that multiple scattering plays a small but non-negligible role in determining sticking factors for atom-surface combinations where the mass ratio is greater than one.

For mass ratios less than one, the predictions of the various models are more complicated. Although we have not measured sticking factors for atom-surface combinations with such mass ratios, our procedure may be applied to this more interesting region if a suitable vacuum is obtained. The technique is relatively independent of the chemistry of the incident and surface atoms and thus may be used for a range of atom-surface combinations. The only

requirements are that (1) the mass of the incident atoms is sufficiently different from that of the surface atoms that they can be resolved by backscattering, (2) the mass of the incident atom is greater than the mass of the ion used for backscattering and (3) the incident atom is not rapidly desorbed at the temperature used for these measurements.

As a technique for the calibration of catcher foils in sputtering experiments, our procedure is quite successful. Although the pressures involved in the sputtering runs were too high to allow us to obtain reliable sticking factors for the Al_2O_3 surfaces, these pressures are typical of those used in sputtering measurements and are thus appropriate for collector foil efficiency calibration. Our measurements indicate that, for our geometry and catcher foils, sputtered atoms of Nb and Rh are collected with almost 100% efficiency. Of course, further measurements are necessary for other elements.

With an improved vacuum, it will be interesting to compare sticking factors obtained from clean foils with those from gas-covered foils. Although sticking factors near one are expected for heavy atoms incident on a lighter surface, such mass ratios are not always obtainable in sputtering experiments. For example, once a fraction of a monolayer of material has been deposited by the sputtering of an alloy, atoms from the lighter component may collide with heavier atoms already deposited on the surface. If sticking is enhanced by a surface gas layer, an improved vacuum might, in fact, be undesirable for certain sputtering measurements since a large sticking factor is desired.

A variety of other sticking factor measurements may be made with minor adaptations to our technique. Such measurements would be of interest in connection with many physical problems ranging from surface physics to astrophysics.

REFERENCES

1. A. T. Modak and P. J. Pagni, J. Chem. Phys. 59, 2019 (1973).
2. L. Trilling and A. Hurkmans, Surf. Sci. 59, 361 (1976).
3. A. Hurkmans, E. G. Overbosch, D. R. Olander and J. Los, Surf. Sci. 54, 154 (1976).
4. A. Hurkmans, E. G. Overbosch and J. Los, Surf. Sci. 62, 621 (1977).
5. R. Sau and R. P. Merrill, Surf. Sci. 34, 268 (1973).
6. S. Tomoda, K. Kumasabura and I. Kusunoki, Surf. Sci. 45, 657 (1974).
7. A. Y. Cho and C. D. Hendricks, J. Appl. Phys. 40, 3339 (1969).
8. K. G. Libbrecht, J. E. Griffith, R. A. Weller and T. A. Tombrello, submitted to Rad. Eff. (1979).
9. H. M. Loebenstein, D. W. Mingay and C. S. Zaidins, Nucl. Instr. and Meth. 33, 175 (1965).
10. A. Hurkmans, E. G. Overbosch and J. Los, Surf. Sci. 59, 488 (1976).
11. E. G. Overbosch, A. Hurkmans and J. Los, Surf. Sci. 63, 417 (1977).

TABLE I

Absolute sticking probabilities for sputtered atoms of Rh and Nb incident on Al_2O_3 collecting surfaces. The integrals I_1 and I_2 are related to the numbers of atoms deposited on the primary and secondary collectors, respectively (see text). $k_A^A(n_1)$ is the sticking probability for atoms of A when the primary collector is thickly coated with atoms of A. $k_B^A(0)$ is the sticking probability for atoms of A on a surface of material B that has collected only a negligible number of A atoms.

A	I_1	I_2	I_2/I_1	$k_B^A(0)$	$k_A^A(n_1)$
Rh	$(1.5 \pm 0.2) \times 10^{16}$	$(6.6 \pm 1.2) \times 10^{14}$	0.046 ± 0.010	$0.95^{+0.05}_{-0.08}$	0.95 ± 0.01
Nb	$(4.1 \pm 0.4) \times 10^{16}$	$(1.3 \pm 0.2) \times 10^{14}$	0.032 ± 0.006	$0.97^{+0.03}_{-0.08}$	0.97 ± 0.01

FIGURE CAPTIONS

FIGURE 1. Geometry for absolute sticking probability measurements. Low-energy atoms are produced by sputtering a target of material A. Some of these sputtered atoms strike the primary catcher foil (material B) where they stick with a probability k_B^A. Many atoms which bounce off strike the cylindrical secondary catcher foil where they may also stick. If the surface density of collected material is not too large, k_B^A may be determined by analysis of these two catcher foils.

FIGURE 2. Geometry for determining the dependence of the sticking probability on the thickness of the collected layer. When the target is sputtered by a given charge, Q, of incident ions, a distribution, $n(\Theta)$, of sputtered atoms is collected on the catcher foils. This distribution is proportional to Q and to the relative sticking probability, $k_B^A(n)$. By obtaining several distributions, $n_i(\Theta)$, corresponding to different sputtering charges, Q_i, the dependence of the sticking probability on layer thicknesses may be determined.

FIGURE 3. Geometry for backscattering analysis. Catcher foils from the sputtering runs are mounted on the sides of a hexagonal target holder which may be raised, lowered or rotated. The target is irradiated with a heavy-ion beam and ions scattered from the target at a lab angle of 147.8° are detected by a surface barrier detector. The detector subtends a solid angle of 6.0×10^{-3} sr.

FIGURE 4. Relative sticking probability for Nb on Al_2O_3. x's refer to values of n_o for which the relative sticking factor is defined to be 1. Statistical errors on the other data points are $\pm 5\%$, and the total error is estimated to be $\pm 8\%$. Within that limit (given by the dashed lines), there is no apparent change in the sticking factor as a function of thickness.

FIGURE 5. Relative sticking factor for Rh on Al_2O_3. As for the Nb data, there is no apparent change in the sticking factor within an estimated error of ±8% (given by the dashed lines).

FIGURE 6. Distribution of material collected on primary catcher foil for Rh on Al_2O_3. These data were fitted to a polynomial in r^2 in order to obtain the integral I_1. Similar data were obtained from the Nb measurement.

FIGURE 7. Distribution of material collected on secondary catcher foil for Rh on Al_2O_3. These data were fitted to a function of the form $\cos^m \chi$. When all data points are included in the fit, $m \approx 0.75$. Similar data were found for the Nb measurement. In both cases, the integral did not depend strongly on the value of m.

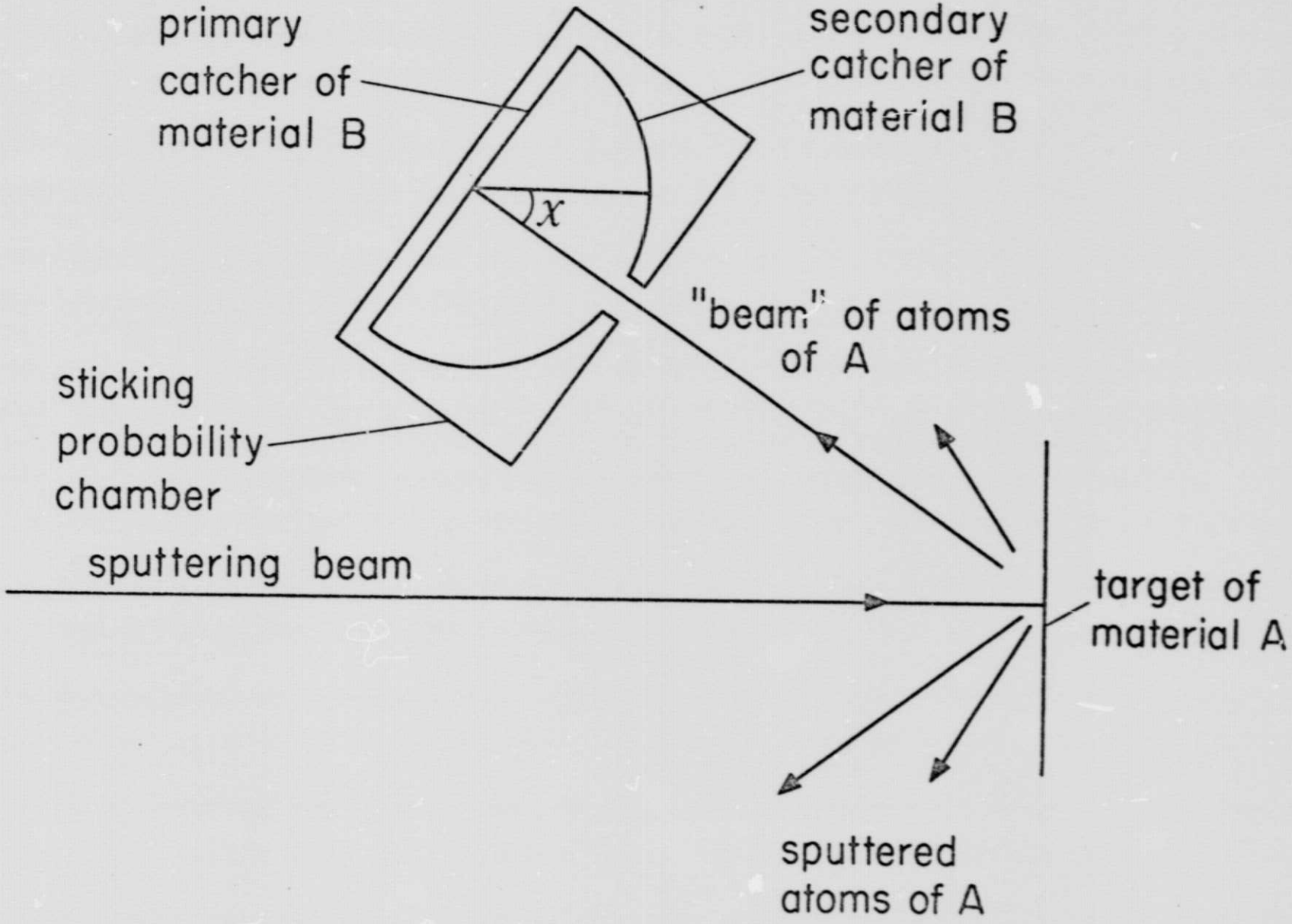
primary
catcher of
material B
secondary
catcher of
material B
x
"beam" of atoms
of A
sticking
probability
chamber
sputtering beam
target of
material A
sputtered
atoms of A

Fig. 1

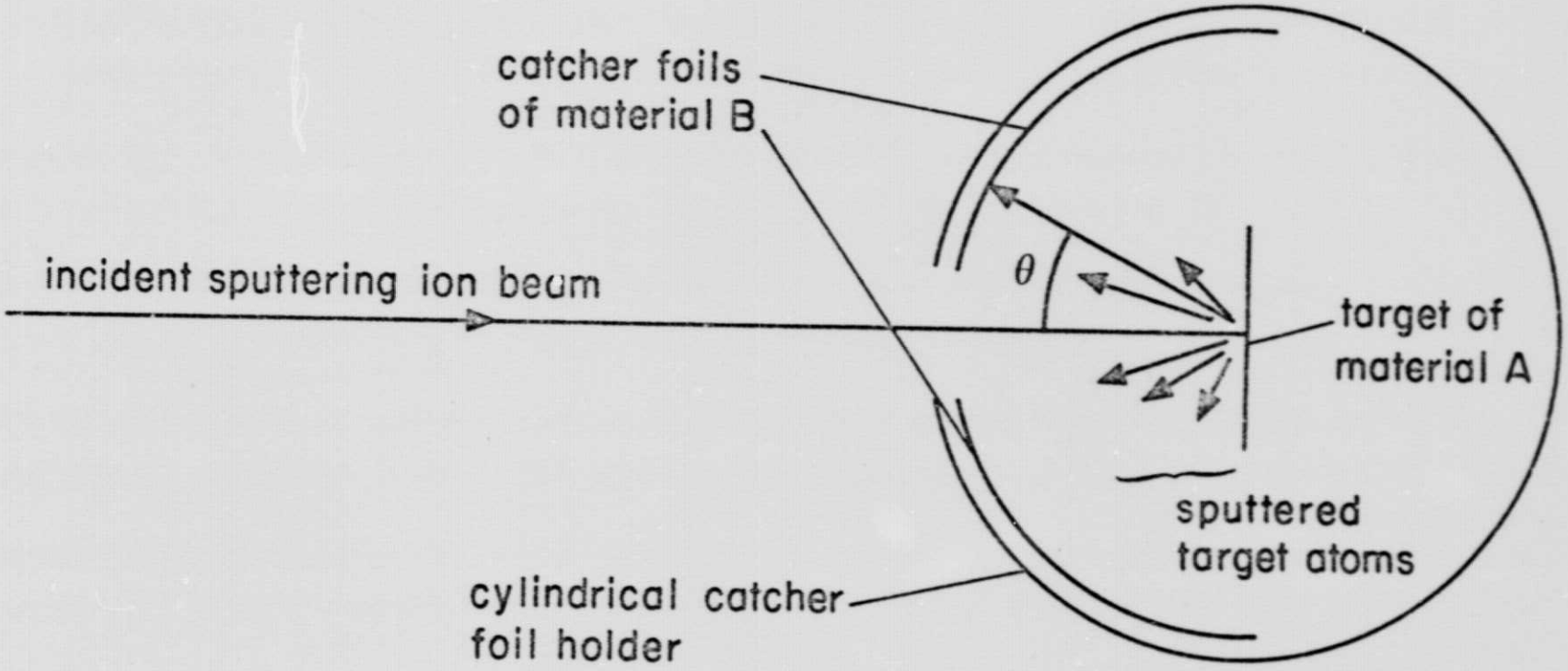
catcher foils
of material B
incident sputtering ion beam
θ
target of
material A
sputtered
target atoms
cylindrical catcher
foil holder

Fig. 2

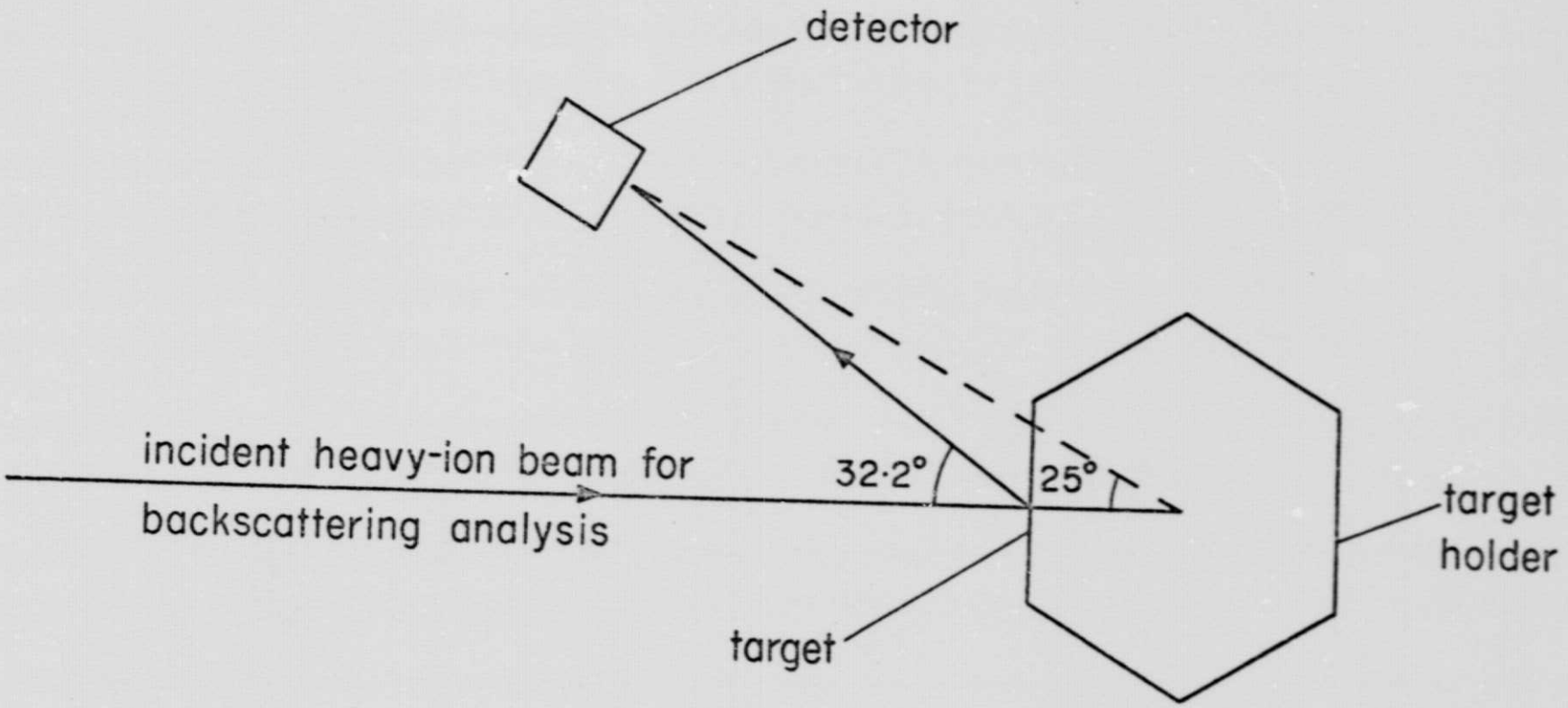
detector
incident heavy-ion beam for
backscattering analysis
32·2°
25°
target
target
holder

Fig. 3

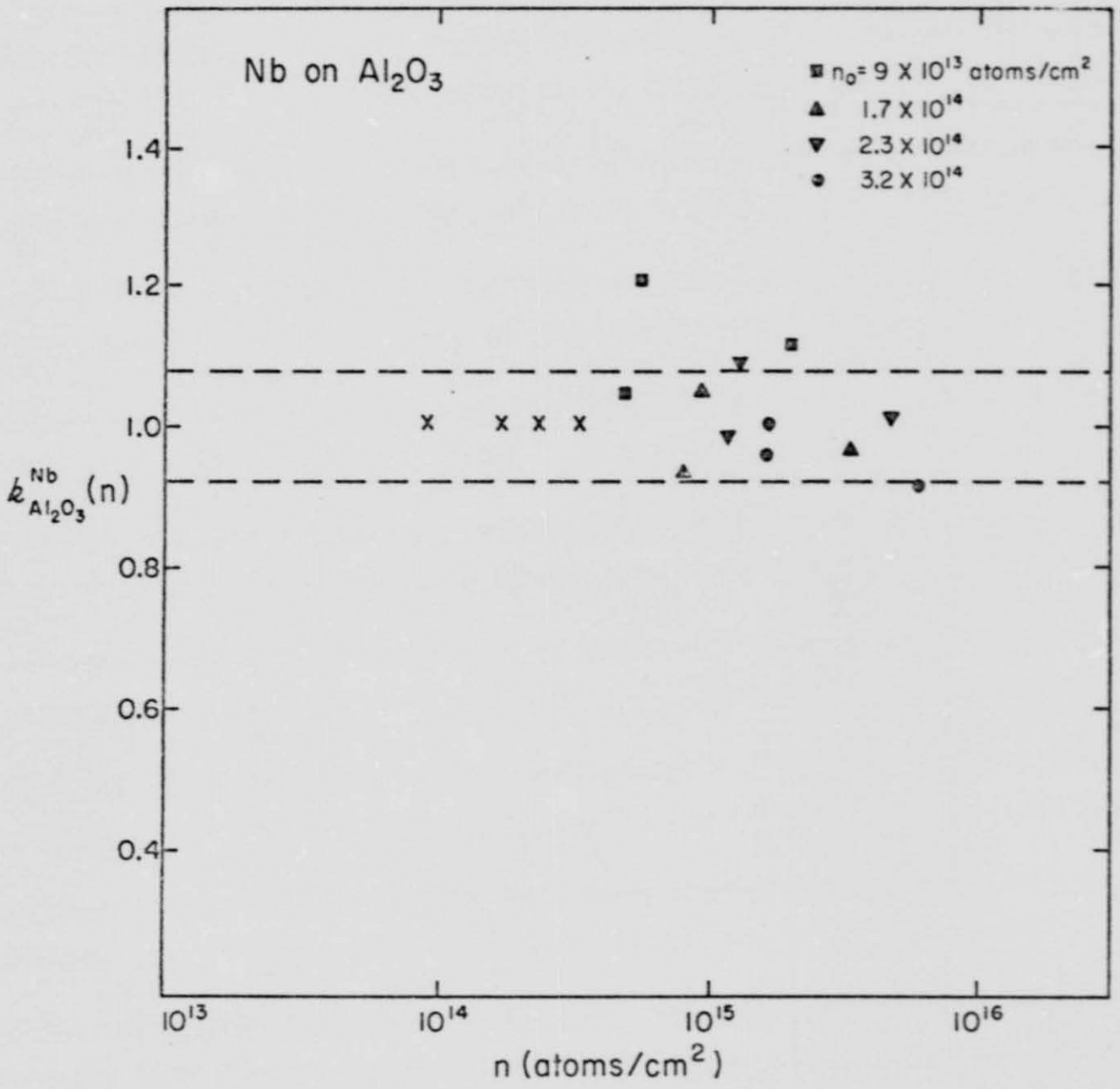
Nb on Al_2O_3
n_0= 9 X 10^{13} atoms/cm^2
1.7 X 10^{14}
2.3 X 10^{14}
3.2 X 10^{14}
1.4
1.2
1.0
0.8
0.6
0.4
$k^{Nb}_{Al_2O_3}(n)$
10^{13}
10^{14}
10^{15}
10^{16}
n (atoms/cm^2)

Fig. 4

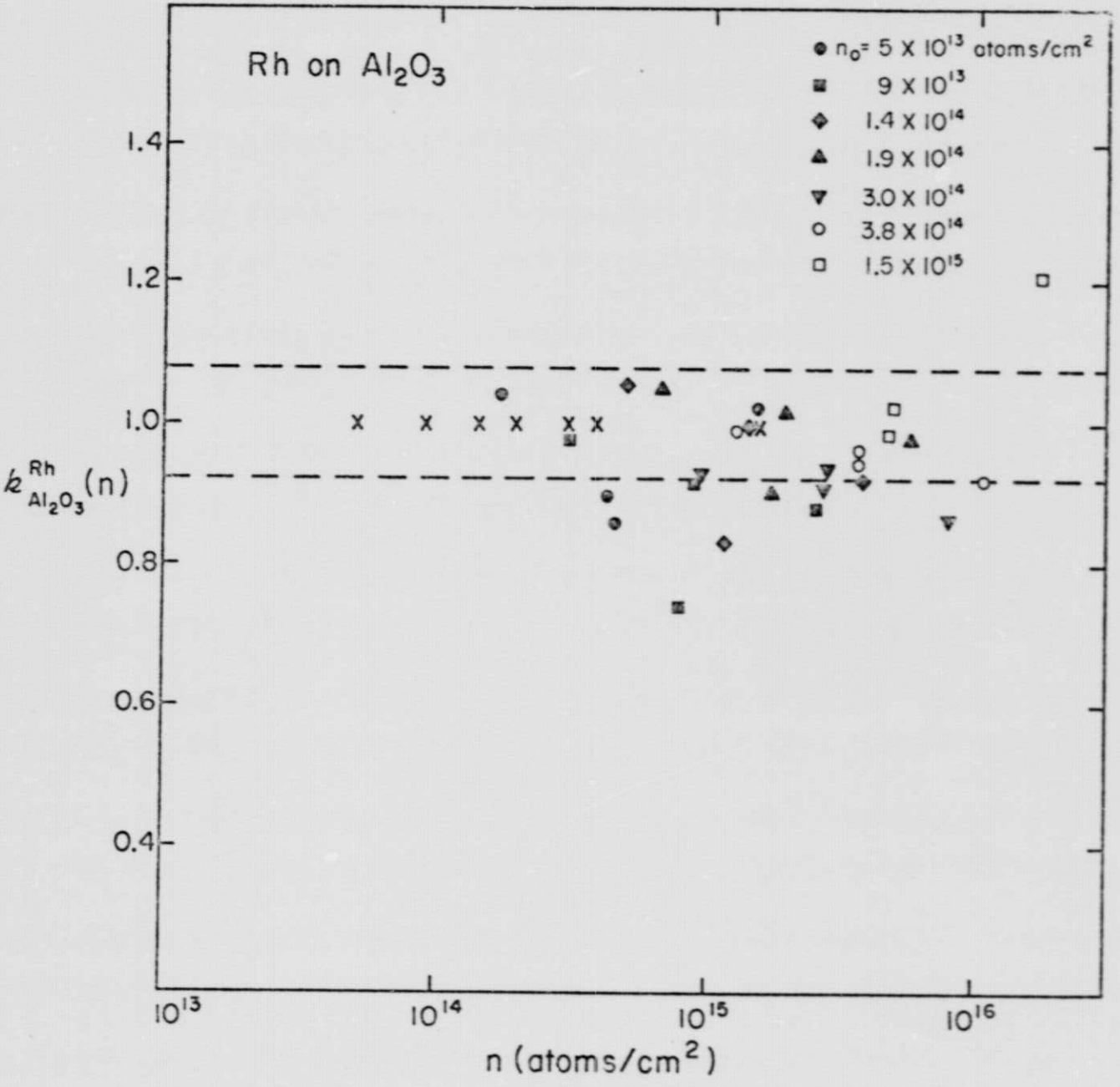
Rh on Al_2O_3
n_o= 5 X 10^{13} atoms/cm^2
9 X 10^{13}
1.4 X 10^{14}
1.9 X 10^{14}
3.0 X 10^{14}
3.8 X 10^{14}
1.5 X 10^{15}
1.4
1.2
1.0
0.8
0.6
0.4
$k^{Rh}_{Al_2O_3}(n)$
10^{13}
10^{14}
10^{15}
10^{16}
n (atoms/cm^2)

Fig. 5

Fig. 6

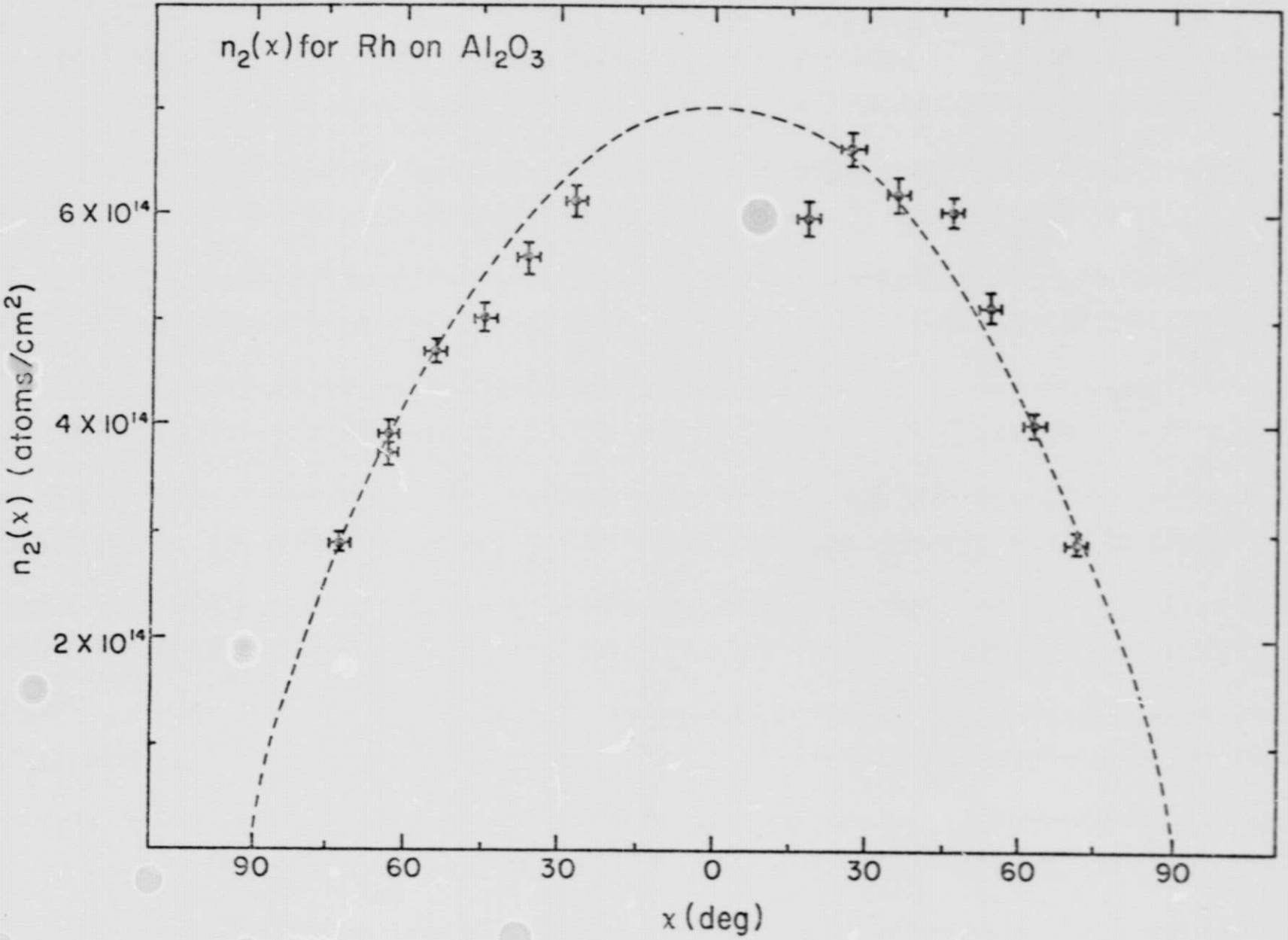
$n_2(x)$ for Rh on Al_2O_3
6×10^{14}
4×10^{14}
2×10^{14}
$n_2(x)$ (atoms/cm^2)
90
60
30
0
30
60
90
x (deg)

FIG. 7